Surface-state scattering by adatoms on noble metals: *Ab initio* calculations using the Korringa-Kohn-Rostoker Green function method

Samir Lounis,* Phivos Mavropoulos, Peter H. Dederichs, and Stefan Blügel

Institut für Festkörperforschung, Forschungszentrum Jülich, D-52425 Jülich, Germany

(Received 23 December 2005; revised manuscript received 13 April 2006; published 24 May 2006)

When surface-state electrons scatter at perturbations, such as magnetic or nonmagnetic adatoms or clusters on surfaces, an electronic resonance, localized at the adatom site, can develop below the bottom of the surface-state band for both spin channels. In the case of adatoms, these states have been found very recently in scanning tunneling spectroscopy experiments for the Cu(111) and Ag(111) surfaces. Motivated by these experiments, we carried out a systematic theoretical investigation of the electronic structure of these surface states in the presence of magnetic and nonmagnetic atoms on Cu(111). We found that Ca and all $3d$ adatoms lead to a split-off state at the bottom of the surface band which is, however, not seen for the sp elements Ga and Ge. The situation is completely reversed if the impurities are embedded in the surface: Ga and Ge are able to produce a split-off state whereas the $3d$ impurities are not. The resonance arises from the s state of the impurities and is explained in terms of strength and the interaction nature (attraction or repulsion) of the perturbing potential.

I. INTRODUCTION

At crystal surfaces the symmetry is lowered: The three-dimensional periodicity in the bulk is lowered to the two-dimensional periodicity at the surface. This leads to the occurrence of two-dimensional surface states,[1,2] which are spatially confined at the surface, since their wave functions decay into the crystal and are strongly damped in the vacuum. Surface states can exist only in regions of the two-dimensional Brillouin zone, where bulk Bloch states are not allowed. They are characterized by a two-dimensional Bloch vector $\vec{k}_\parallel$ in this surface Brillouin zone, which describes the propagation in the surface plane. A projection of the bulk band structure to the surface plane can result in $\vec{k}_\parallel$ regions, where bulk states are forbidden. In these gaps of the projected bulk band structure surface states can occur provided that their energy is lower than the work function. These two conditions guarantee that the wave functions of the surface states decay exponentially both into the crystal and into the vacuum region. Moreover, we note that for Cu(111), the subject of the present work, the surface band minimum lies below the Fermi energy.

Recently, strong interest arose concerning an important physical effect associated with the interaction of a two-dimensional surface state with the states of an adatom. It was shown that for Cu adatoms on Cu(111) a bound state splits off from the bottom of the Cu(111) surface state.[3,4] This effect was basically predicted by Simon[5] who stated that in two-dimensional free space any attractive potential has a bound state. Gauyacq *et al.*[6] suggested that an adatom-induced localization of the surface state may be observed in scanning tunneling spectroscopy (STS) as a peak appearing just below the surface band edge when a Cs adatom is deposited on Cu(111).

Using low-temperature STS, Limot *et al.*[3] investigated silver and cobalt adatoms on Ag(111) as well as copper and cobalt adatoms on Cu(111). The bound state appears both for magnetic and nonmagnetic adatoms. Moreover, using a Newns-Anderson model the authors explained the results as arising from the coupling of the adatom's orbital (which was supposed to be the s orbital) with the surface-state electrons, and being broadened by the interaction with bulk electrons of the same energy. On the other hand, Olsson *et al.*[4] used the same type of experiment and performed pseudopotential calculations for single Cu adatoms on Cu(111). The calculated local density of states (LDOS) exhibits several adatom-induced peaks. Two of them are assigned to resonances deriving from the d_{z^2} atomic orbital and sp_z hybrid orbitals. The third one corresponds to a localization of the surface state at the adatom without a specified orbital origin. In fact, these adatom-induced peaks appearing at the bottom of the surface state were already observed by another experiment,[7] again without a clear assignment of their origin. Davis *et al.*[8] have observed similar localized states in STS measurements for Cr atoms in the surface layer of the Fe(001) surface. *Ab initio* calculations of Papanikolaou *et al.*[9] confirmed this and showed that similar localized states occur for many other impurities in the Fe(001) surface.

In this work we study the origin and the condition of existence for such an impurity-induced split-off state on the Cu(111) surface. For this purpose we have performed *ab initio* calculations using the Korringa-Kohn-Rostoker (KKR) Green function method for impurities on the Cu(111) surface. We consider single impurities of the $3d$ and $4sp$ elements as adatoms on the Cu(111) surface and as impurities in the first layer. We find that split-off states can appear both for adatoms on the surface as well as for substitutional impurities in the surface. In the case of magnetic impurities these states always appear in both spin channels and show a very small spin splitting.

II. COMPUTATIONAL ASPECTS

In the present work we use the full-potential KKR Green function method.[10] This method is ideal for treating systems involving impurities on or in surfaces and in bulk crystals.

195421-1

Within the KKR method the impurities are described by considering a cluster of perturbed atomic potentials which includes the potentials of the impurities and the perturbed potentials of several neighbor shells. Also in the vacuum region the space is filled by cellular potentials, of which the ones close to the impurity are perturbed. The impurity potential and the perturbed potentials of the neighboring cells are embedded in an otherwise ideal unperturbed surface.

The KKR method is based on the multiple-scattering theory. For nonoverlapping potentials the following angular momentum representation of the Green's function $G(\mathbf{r}+\mathbf{R}_n,\mathbf{r}'+\mathbf{R}_{n'};E)$ can be derived:

$$G(\mathbf{r}+\mathbf{R}_n,\mathbf{r}'+\mathbf{R}_{n'};E) = -i\sqrt{E}\sum_L R_L^n(\mathbf{r}_<;E)H_L^n(\mathbf{r}_>;E)\delta_{nn'}$$

$$+ \sum_{LL'} R_L^n(\mathbf{r};E)G_{LL'}^{nn'}(E)R_{L'}^{n'}(\mathbf{r}';E). \tag{1}$$

Here E is the energy and $\mathbf{R}_n$, $\mathbf{R}_{n'}$ refers to the atomic positions. $\mathbf{r}_<$ and $\mathbf{r}_>$ denote, respectively, the shorter and longer vectors $\mathbf{r}$ and $\mathbf{r}'$ which define the position in the Wigner-Seitz cell centered around $\mathbf{R}_n$ or $\mathbf{R}_n'$. The $R_L^n(\mathbf{r};E)$ and $H_L^n(\mathbf{r};E)$ are, respectively, the regular and irregular solution of the Schrödinger equation.

The structural Green functions $G_{LL'}^{nn'}(E)$ are then obtained by solving the Dyson equation for each spin direction

$$G_{LL'}^{nn'}(E) = \mathring{G}_{LL'}^{nn'}(E) + \sum_{n'',L''L'''} \mathring{G}_{LL''}^{nn''}(E)\Delta t_{L''L'''}^{n''}(E)G_{L'''L'}^{n''n'}(E). \tag{2}$$

The summation in (2) is over all lattice sites n'' and angular momenta L'', L''' for which the perturbation $\Delta t_{L''L'''}^{n''}(E) = t_{L''L'''}^{n''}(E) - \mathring{t}_{L''L'''}^{n''}(E)$ between the t matrices of the real and the reference system is significant. $\mathring{G}_{LL'}^{nn'}$ are the structural Green function of the reference system, i.e., in our case the ideal Cu(111) surface.

We have carried out our calculations in the local spin density approximation (LSDA) with the parameters of Vosko *et al.*[12] Angular momenta up to $l_{max}=3$ are included in the expansion of the wave functions and up to $2l_{max}=6$ in the charge density expansion. We have checked these cut-offs to be adequate for our purpose.

First, the surface Green functions were determined for the surface of Cu(111). The lattice LSDA equilibrium parameter was used (6.63 a.u. $\approx$ 3.51 Å). To describe the impurities on the surface, we consider a cluster of perturbed potentials which includes the potentials of the impurities and the perturbed potentials of several neighbors shell, with a typical size of 29 perturbed sites for the adatoms. All adatoms are assumed to sit at the hollow position in the first vacuum layer. In the following, we take as reference energy the Fermi level E_F.

According to the Tersoff-Hamann model[13] the scanning tunneling spectra can be related to the s DOS induced by the surface or by the adatom at the position of the STS tip.
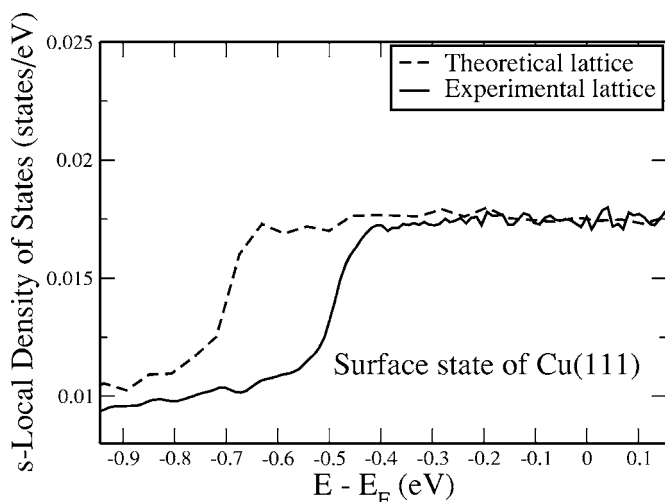

FIG. 1. s local density of states (LDOS) at the second vacuum layer above the Cu(111) surface. The full line represents the s LDOS with the experimental lattice parameter and the dashed line refers to the s-LDOS with the LDA lattice constant.

Adopting this model, we calculate the s LDOS at a distance $z=2.86$ Å directly above the adatom. This corresponds to a lattice position in the third vacuum layer above the surface.

III. RESULTS

A. Surface state of Cu(111)

The first step of our work consists in calculating the energy of the bottom of the surface state. As depicted with the dashed line in Fig. 1, the s LDOS is characterized by a surface state which appears at -0.68 eV below the Fermi energy. We note that experimentally, this threshold energy is higher and is situated at -0.45 eV.[14] This inconsistency is due to the LDA equilibrium lattice parameter (3.51 Å) we used since a test calculation with the experimental lattice parameter (3.62 Å) gives a value of -0.49 eV for the threshold energy (see the full line in Fig. 1). Note that for two-dimensional bands the LDOS shows a jump at the energy of a band minimum or maximum, which is slightly broadened in Fig. 1 due to the use of a small imaginary part for the energies.

B. 3d impurities as adatoms

Results. The calculated LDOS for 3d adatoms presented in Fig. 2 exhibit several adatom-induced peaks. The LDOS refer to an unoccupied *lattice position* in the third vacuum layer above the surface, i.e., 2.86 Å above the single adatoms in the first vacuum layer. We focused on the region where the split-off state appears experimentally, i.e., around the bottom of the surface state, which, as stated above, is in our calculations located at -0.68 eV.

Let us start with a Cu adatom. Below E_F, Fig. 2 shows that two states appear in the LDOS. The first one [see arrow (a) in Fig. 2] is a split-off state situated at the bottom of the surface state (≈ -0.68 eV) as was already found by Limot *et al.*[3] and by Olsson *et al.*[4] To understand the origin of the
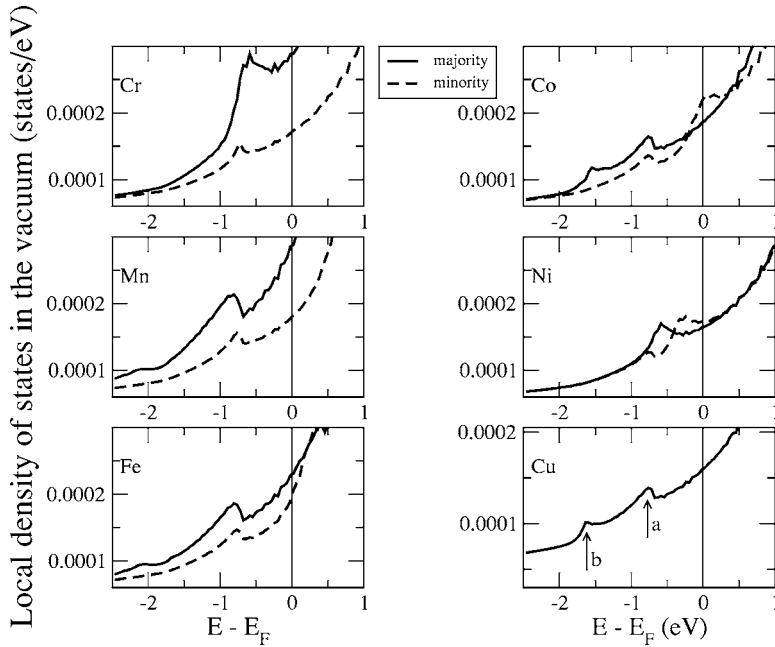
FIG. 2. LDOS at the second vacuum layer above the 3d adatoms (2.86 Å) on the Cu(111) surface. The full lines refer to majority-spin states, the dashed lines to minority-spin ones. The two arrows show the protrusions discussed in the text: (a) corresponds to a split-off state, (b) is a d_{z^2} resonance.

second protrusion [see arrow (b)] we plot in Fig. 3 the d-partial LDOS of the adatoms which show that it comes from a resonance of the d_{z^2} state at ≈ -1.7 eV.

For all the 3d adatoms examined, we find for both spin directions a peak in the LDOS in the region below the threshold value of the surface state. However, we also find peaks at other energies, e.g., for Cu at -1.7 eV as mentioned earlier and for Co at -1.5 eV for spin-up and at around 0 eV for spin-down states. In order to understand this behavior, we have to in the first place understand the electronic and magnetic properties of the impurities and then which of the im-

purity states penetrate well into the vacuum, such that they show up in the LDOS of the second layer and can be detected by the STM.

Let us first address the second question. In the vacuum region, states with small in-plane $\vec{k}$-components $k_{\parallel}$ decay most slowly as a function of the perpendicular distance z from the surface. In fact, for a given energy $E = -\chi^2$ below the vacuum barrier, a wave function with in-plane component $k_{\parallel}$ decays as $e^{-(\chi^2 + k_{\parallel}^2)^{1/2} z}$. Therefore states with small $k_{\parallel}$ values decay slowest; for higher $k_{\parallel}$ a part of the kinetic energy is used for in-plane oscillations. Since the states with $k_{\parallel}=0$ show no in-plane oscillations and exhibit the full symmetry of the surface, we find that for the (111) surface states with s, p_z, and d_{z^2} show a slow decay in the vacuum region and can be well seen in STM, while other p and d states are strongly attenuated. An analogous argument holds for single adatoms on the (111) surface, since only these states exhibit the full point symmetry of the adatom-on-surface configuration,[9] and have thus no oscillations to use as a part of the kinetic energy.

To understand the magnetic properties of the adatoms, we have plotted in Fig. 3 the d contribution to the LDOS at the adatom site. For the Cu adatom, we find a sharp d peak at -1.7 eV, i.e., at the edge of the bulk d, band of Cu. This is a consequence of the repulsive potential, which the Cu adatom experiences in the first layer, shifting the d states to higher energies than in the bulk. All other impurities are magnetic and exhibit sizable moments, leading to a spin splitting of the so-called virtual bound states. For the different adatoms, the calculated local moments M_s are Cr (4.06μ_B), Mn (4.28μ_B), Fe (3.21μ_B), Co (1.96μ_B), and Ni (0.34μ_B). Note that the spin splitting is roughly given by IM_s, where I is the exchange integral of the order of 1 eV.[11] In the case of the Cr adatom, the minority peak is at higher energies and cannot be seen in Fig. 3, while for Fe and Mn the majority peaks are at lower energies.
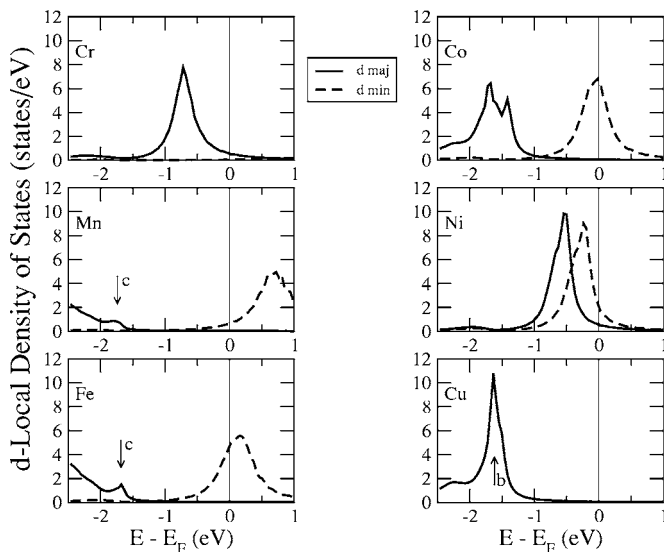

FIG. 3. d contributions to the LDOS of 3d adatoms on the Cu(111) surface. The full lines describe the majority-spin states and the dashed lines describe the minority-spin states. Since the Cu adatom is nonmagnetic, the majority and minority virtual bond states coincide.
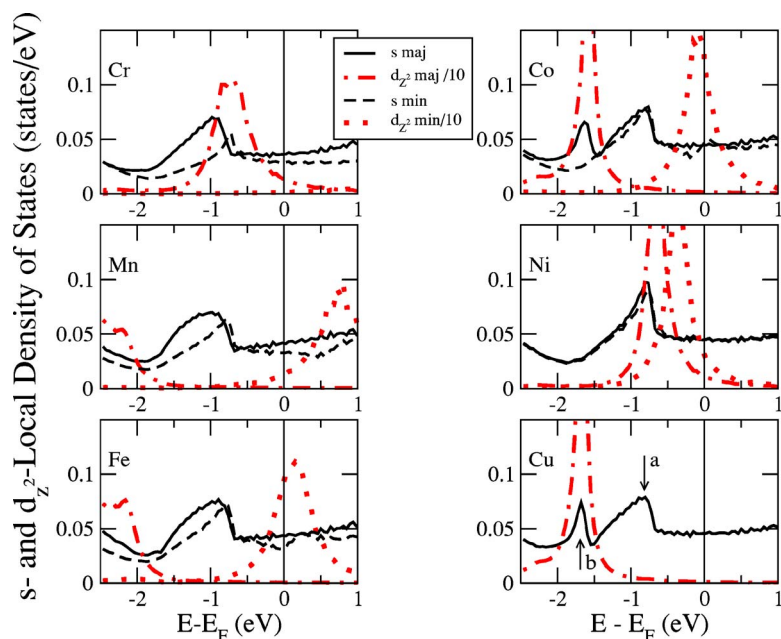
FIG. 4. (Color online) Focus on the *s*-partial LDOS of the impurity atoms and d_{z^2}-partial LDOS reduced by a factor of 10. Black full lines represent the majority spin of *s*-partial LDOS, red (dark gray) dashed-dotted lines represent the majority spin of *d*-partial LDOS, black dashed lines describe the minority spin of *s*-partial LDOS, and red (dark gray) dotted lines describe the minority spin of *d*-partial LDOS.

Interpretation. Let us now come back to the interpretation of Fig. 2, showing the LDOS in the second vacuum layer, at the position above the adatom, for majority and minority electrons. Independently of the peak structure, we observe a general increase of the DOS at higher energies, which arises from the increase of the spatial extent of the wave functions for larger energies. For Cu, the peak at −1.7 eV coincides with the d_{z^2} peak in the local DOS of the adatom, shown in Fig. 3. For clarification we show in Fig. 4 the local *s* DOS and the d_{z^2} DOS of the adatoms (the latter reduced by a factor of 10). For Cu, as well as for the majority states of Co, we see a maximum and minimum in the *s* LDOS at the d_{z^2}-peak position, arising from the Fano-like resonant scattering of the *s* states at the d_{z^2} resonance. This effect cannot occur for a single adatom in free space or in jellium, since the *s* and *d* orbitals are orthogonal. Therefore, it is brought about by the reduced symmetry, i.e., the scattering at the substrate atoms. The LDOS peak below −0.68 eV [arrow (a)] is the split-off state of the Cu adatom, induced by the attractive nature of the adatom potential in the first vacuum layer. The same states are also seen for the Co adatom, more or less identical for both spin directions. In addition we see for the minority *s* state of Co a Fano-like resonance behavior at the Fermi level, arising from the interaction with the minority d_{z^2}-virtual bound states.

In the case of the Ni adatoms the virtual bound states for the two spin directions are only weakly split and more or less coincide with the energy level of the split-off surface state. Therefore, in the local *s* DOS the two effects, the formation of the split-off state and the resonant scattering at the d_{z^2} resonances, cannot be distinguished. However, in the vacuum region (Fig. 2) the spin splitting of the majority and minority d_{z^2} states can be clearly seen.

For Fe-, Mn- and Cr adatoms another effect can be seen in the vacuum LDOS (Fig. 2) and the local *s* DOS in Fig. 4. The intensity in the majority split-off surface state is considerably higher than for the minority state. This can have several reasons. For instance, due to the exchange splitting the

majority potential is somewhat stronger than the minority one, leading to a smaller lateral extension of the split-off states and to a larger intensity on the adatom site. In particular, in the case of Cr, also the resonant interaction with the impurity d_{z^2} virtual bound state becomes important, strongly increasing the majority intensity on the impurity site as well as in vacuum.

Moreover, we have noticed a small peak appearing in the Mn- and Fe-adatom majority *d* LDOS [see arrow (c) in Fig. 3] at the same position where the virtual bound states of Cu-adatom is situated ($\approx$−1.7 eV). However, these protrusions have a different origin since there is no peak at −1.7 eV in the d_{z^2} LDOS for Mn- and Fe-adatom contrary to Cu or Co adatoms (see Fig. 4). They appear at the remaining *d*-partial LDOS (d_{xy}, d_{yz}, d_{xz}, and $d_{x^2-y^2}$) which are strongly damped in the vacuum. For symmetry reasons they do not hybridize with the *s* LDOS explaining thus why we do not see a peak at the *s* LDOS of Mn and Fe adatoms contrary to Cu and Co adatoms. We believe, however, that these peaks can be interpreted as split-off states from a surface state at the $\bar{M}$ point,[15] which shows a negative dispersion, such that a repulsive impurity potential leads for these *d* states to a split-off state at higher energies, i.e., above the corresponding surface band.

C. *sp* impurities as adatoms

Results. We consider now some *sp* impurities as adatoms, for which the behavior is not complicated by the spin-polarized *d* states. As a first candidate we consider Ca at the beginning of the 3*d* series. The calculations give a well-defined split-off state at the same position as for Cu and the 3*d* impurities, i.e., below the minimum of the surface band. In addition we performed calculations for Zn, Ga, and Ge adatoms. The split-off state is still seen for Zn but not anymore for Ga and Ge atoms.

Interpretation. The reason for this is that in the LDOS of Ga and Ge adatoms the *s* states have moved to lower ener-
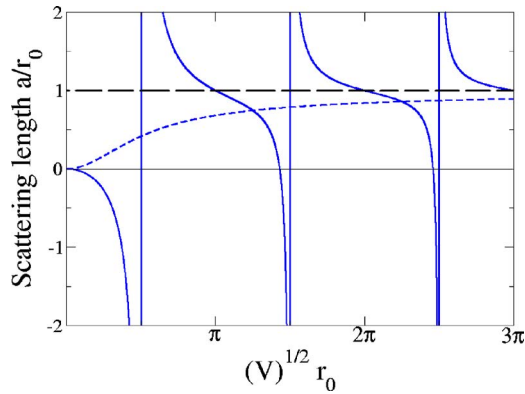
FIG. 5. (Color online) Variation of the scattering length a versus the potential. Full lines correspond to a negative potential while the blue short-dashed line describes the case of positive potential (always repulsive). The figure is obtained for a small positive energy value and an elastic s scattering by a rectangular spherical potential well of depth V and radius r_0.

gies below the surface-state minimum. In this case the s scattering at the adatoms becomes effectively repulsive, so that no split-off state occurs. To explain this we note that the scattering behavior of a scattering center is directly related to the t matrix, and only indirectly to the potential. Our results are in contradiction with the usual statement that any attractive potential leads to a split-off state of a two-dimensional surface state. This is not correct in our case, since the t matrix of the adatom is basically a three-dimensional quantity. For s scattering at low energies $E \sim 0$, the t matrix is related to the so-called scattering length a, being discussed in many books on quantum mechanics. The quantity a is the length where the extrapolation of the asymptotic form of the wave function for $E=0$ vanishes. For the simple model of spherical potential well of depth V and radius r_0 the scattering length a is plotted in Fig. 5. For a repulsive potential the scattering length is positive and approaches the well radius r_0 for large V. For a weakly attractive potential a is negative. However, when the potential V becomes stronger and attractive, the scattering length assumes even stronger negative values, until it jumps at a critical strength $V=V_0$ from $-\infty$ to $+\infty$, and is positive for further increased V values. At the critical strength V_0 a bound state appears at $E=0$, moving to lower energies for further increased negative V values, and making the scattering length positive as for a repulsive potential. To compare with the real situation of the adatoms, the potential of the transition metal atoms is sufficiently weak so that a split-off state exists, since the atomic $4s$ level is far above the Fermi level and the scattering length is negative. However, for the Ge adatom the $4s$ level has moved below the minimum of the surface state, so that the scattering length is positive and no split-off state appears. When progressing further in the atomic table a split-off state can only appear again, when in the next series of the elements, say from Rb to Ag, the $5s$ level has moved down towards the Fermi level.

D. Impurities in the surface layer

The scattering of the surface states at impurities in the first surface layer is basically different from the scattering at
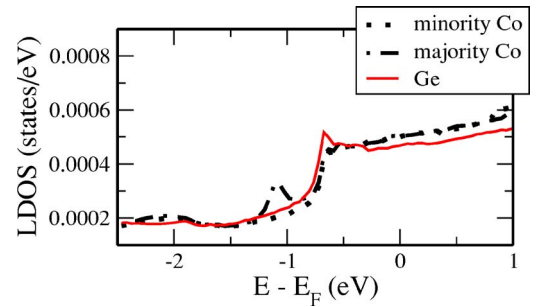

FIG. 6. (Color online) LDOS in vacuum at the second layer above the impurities which are sitting in the surface layer. One can see the appearance of the split-off state above Ge impurities in a red (dark gray) full line but not above Co (black dotted-dashed line). Above the last one, a protrusion appears at ≈ -1.1 eV on the majority-spin channel which is due to the d state of the Co impurity.

adatoms, since the effective potential for scattering is the difference between the potential of the impurity and the potential of the substituted Cu atom. Therefore all $3d$ impurities in the first layer do not show any split-off surface state, since the potential difference is very small (and moreover slightly repulsive). On the other hand for Ge impurities in the first layer, the calculations yield a split-off state, as is shown by the small peak in Fig. 6. Apparently the difference in potential is sufficiently attractive, such that a weakly localized state is formed. Therefore we obtain the opposite trend than for the adatoms. Transition metal impurities exhibit a split-off surface state as adatoms, but not as substitutional impurities in the first layer, whereas for Ga and Ge just the opposite is true.

IV. LIMITATIONS OF THE LSDA

We now discuss the limitations of our calculations, in particular, concerning the Kondo effect which cannot be captured by the LSDA. It is well known that, at low temperatures, the spin moment of the magnetic impurities fluctuates, so that these appear nonmagnetic. The temperatures at which the experiments are conducted are in many cases below the Kondo temperature; e.g., a characteristic Kondo feature in the spectra was observed for Co on Cu in Ref. 3

The Kondo effect is characterized by a narrow Abrikosov-Suhl resonance of the DOS at E_F which is absent in our calculations. However, the split-off states are well below E_F. Furthermore, the split-off states appear by the interaction of impurity s states with the surface band while the Abrikosov-Suhl resonance is due to the interaction of the localized impurity d states with the conduction electrons. Therefore, our results on the split-off state are physically relevant.

On the other hand, the spin-dependent spectra of the magnetic impurities should be corrected towards an averaging of the two spin channels, if the temperature is below the Kondo temperature. Although the Kondo fluctuations kill the magnetic moment, the splitting of the d virtual bound states remains, corresponding to the single and double occupancy of the impurity local state.

V. SUMMARY

We have performed self-consistent calculations on single impurities deposited on a Cu(111) surface in order to inves-

tigate the split-off state recently seen in experiment.[3,4] We see two kinds of split-off states: One is due to an attractive potential below the $\bar{\Gamma}$ surface state and the other one is due to a repulsive potential above the $\bar{M}$ surface state. We found that Ca, all $3d$, and Zn adatoms produce the first resonance which is not the case for the sp adatoms Ga and Ge. The presence of the split-off state for Ca means that s states have a stronger contribution to its realization then d states. The behavior is totally different if the impurities are embedded in the surface layer. In particular, Ga and Ge lead to a protrusion at the bottom of the surface band. One question addressed in this work is to explain the absence of a split-off state for sp adatoms and $3d$ impurities embedded in the first surface layer. The former case is interpreted in terms of sign change of the scattering length for attractive potentials, which then may act effectively as repulsive potentials. In the latter case, the reference potential is one of the Cu surfaces, which is not too different from the potentials of all $3d$ impurities. Therefore, we do not see any localization.

---

*Electronic address: s.lounis@fz-juelich.de

[1] I. E. Tamm, Z. Phys. **76**, 849 (1932).

[2] W. Shockley, Phys. Rev. **56**, 317 (1939).

[3] L. Limot, E. Pehlke, J. Kröger, and R. Berndt, Phys. Rev. Lett. **94**, 036805 (2005); J. Kröger, L. Limot, H. Jensen, R. Berndt, S. Crampin, and E. Pehlke, Prog. Surf. Sci. **80**, 26 (2005).

[4] F. E. Olsson, M. Persson, A. G. Borisov, J.-P. Gauyacq, J. Lagoute, and S. Fölsch, Phys. Rev. Lett. **93**, 206803 (2004).

[5] B. Simon, Ann. Phys. (N.Y.) **97**, 279 (1976).

[6] J. P. Gauyacq, A. G. Borisov, and A. K. Kazansky, Appl. Phys. A **78**, 141 (2004).

[7] V. Madhavan, W. Chen, T. Jamneala, M. F. Crommie, and N. S. Wingreen, Science **280**, 567 (1998); V. Madhavan, W. Chen, T. Jamneala, M. F. Crommie, and N. S. Wingreen, Phys. Rev. B **64**, 165412 (2001).

[8] A. Davies, J. A. Stroscio, D. T. Pierce, and R. J. Celotta, Phys.

Rev. Lett. **76**, 4175 (1996).

[9] N. Papanikolaou, B. Nonas, S. Heinze, R. Zeller, and P. H. Dederichs, Phys. Rev. B **62**, 11118 (2000).

[10] N. Papanikolaou, R. Zeller, and P. H. Dederichs, J. Phys.: Condens. Matter **14**, 2799 (2002).

[11] O. Gunarsson, J. Phys. F: Met. Phys. **6**, 587 (1976); J. F. Janak, Phys. Rev. B **16**, 255 (1977).

[12] S. H. Vosko, L. Wilk, and M. Nusair, J. Chem. Phys. **58**, 1200 (1980).

[13] J. Tersoff and D. R. Hamann, Phys. Rev. Lett. **50**, 1998 (1983); Phys. Rev. B **31**, 805 (1985).

[14] F. Reinert, G. Nicolay, S. Schmidt, D. Ehm, and S. Hüfner, Phys. Rev. B **63**, 115415 (2001).

[15] A. Euceda, D. M. Bylander, and L. Kleinman, Phys. Rev. B **28**, 528 (1983).